takes place under these extreme conditions. In the presence of air, the Cd atoms were reoxidized to $Cd^{2+}$, the overall process thus being an anodic corrosion.

The near band gap fluorescence was slightly blue-shifted when excited by intense laser light (Figure 13). Under these circumstances, the emission did not occur from a particle carrying just one $e^-$–$h^+$ pair but had been excited by several photons at the same time. The energy level of the exciton in a small CdS particle carrying one or two excess electrons is shifted to shorter wavelengths.[22] We invoke this effect in our explanation of the blue-shift in Figure 13. The extremely short lifetime of the fluorescence upon laser excitation is explained by the strongly increased rate of recombination of the charge carriers due to the high local concentration during the flash.

**Acknowledgment.** The authors express their gratitude for the excellent assistence in the laboratory of M. Weller, for helpful discussions with L. Katsikas, and for advice in the electron microscopic investigations by Dr. B. Tesche and K. Weiss in the Fritz-Haber-Institut, Max-Planck-Gesellschaft.

**Registry No.** CdS, 1306-23-6; (Zn/Cd)S 3:1, 109636-85-3; (Zn/Cd)S 1:1, 39466-56-3; (Zn/Cd)S 1:3, 37246-65-4.

(22) Henglein, A.; Kumar, A.; Janata, E.; Weller, H. *Chem. Phys. Lett.* **1986**, *132*, 133–136.

# Molybdenum(VI) and Molybdenum(V) Complexes with *N,N'*-Dimethyl-*N,N'*-bis(2-mercaptophenyl)ethylenediamine. Electrochemical and Electron Paramagnetic Resonance Models for the Molybdenum(VI/V) Centers of the Molybdenum Hydroxylases and Related Enzymes

**Dulal Dowerah,[1a] Jack T. Spence,*[1a] Raghuvir Singh,[1a] Anthony G. Wedd,[1b] Graham L. Wilson,[1b] Frank Farchione,[1b] John H. Enemark,[1c] John Kristofzski,[1c] and Michael Bruck[1c]**

*Contribution from the Department of Chemistry and Biochemistry, Utah State University, Logan, Utah 84322-0300, the Department of Chemistry, La Trobe University, Bundoora, Victoria 3083, Australia, and The Department of Chemistry, University of Arizona, Tucson, Arizona 85721.*
*Received November 21, 1986*

**Abstract:** As models for the molybdenum(VI/V) centers of the molybdenum hydroxylases and related enzymes, $MoO_2L$ and MoOClL ($LH_2$ = *N,N'*-dimethyl-*N,N'*-bis(2-mercaptophenyl)ethylenediamine) have been synthesized. The structure of $MoO_2L$ has been determined by X-ray crystallography. The compound crystallizes in space group $P2_1/n$, with $a$ = 10.049 (2) Å, $b$ = 14.538 (2) Å, $c$ = 12.143 (1) Å, $\beta$ = 103.73 (1)°, and $Z$ = 4. $MoO_2L$ is six-coordinate with approximate $C_2$ symmetry, with the two thiolate S atoms trans to one another and the two tertiary amine N atoms approximately trans to the terminal oxo groups. $MoO_2L$ undergoes reversible one-electron reduction on both the cyclic voltammetric and coulometric time scales to give various oxo–Mo(V) complexes. The EPR spectra of these complexes, including $^{98}Mo$, $^2H$, and $^{17}O$ substituted species, are consistent with formulation as $[MoO_2L]^-$, *cis*-MoO(OH)L, $[MoOSL]^-$, and *cis*-MoO(SH)L. $^1H$ coupling constants for *cis*-MoO(OH)L (1.65 mT) and *cis*-MoO(SH)L (1.05 mT) and the $^{17}O$ coupling constants for $Mo^{17}O(^{17}OH)L$ (0.25 and 0.82 mT), $[Mo^{17}OSL]^-$ (0.43 mT), and $Mo^{17}O(SH)L$ (0.22 mT) have been measured. MoOClL exhibits reversible one-electron electrochemical reduction in its cyclic voltammogram but decomposes upon coulometric reduction. EPR data indicate it is *trans*-MoOClL. Substitution of $Cl^-$ by $OH^-$, $F^-$, and $SH^-$ has been effected in solution. The implications of the results for the structures of Mo(VI/V) centers of the enzymes are discussed. In particular, $Mo^VOS(OR)$ and $Mo^VO(SH)(OR)$ (OR = bound product) are suggested as the centers responsible for the "very rapid" and "rapid" EPR signals of xanthine oxidase. An $Mo^VO(OH)$ center appears to be involved in the "slow" EPR signal of xanthine oxidase and the low pH forms of sulfite oxidase and nitrate reductase; the high pH forms of the latter enzymes, however, do not appear to involve a conjugate base $Mo^VO_2$ center.

The molybdenum hydroxylases and related enzymes catalyze biological two electron redox reactions in which an oxygen atom or a hydroxyl group is added to or removed from the substrate. The most extensively studied of these enzymes are xanthine oxidase (XO),[2a] xanthine dehydrogenase (XD),[3a] sulfite oxidase (SO),[2a] and nitrate reductase (NR).[2b] The minimal structure of the molybdenum center, as deduced by EXAFS and EPR investigations, for oxidized XO and XD is $Mo^{VI}O(S)(SR)_2$,[3] with an oxo, sulfide, and two thiolate ligands. A $Mo^{VI}O_2(SR)_{2-3}$ center with two oxo and two or three thiolate ligands appears to be present in oxidized SO, in the desulfo form of XD and in oxidized NR from *Chlorella vulgaris*.[3a] Some of the thiolate ligands may be furnished by the molybdenum cofactor, Mo-co.[4] Oxygen, ni-

(1) (a) Utah State University. (b) La Trobe University. (c) University of Arizona.

(2) (a) Hille, R.; Massey, V. In *Molybdenum Enzymes*; Spiro, T. G.; Ed.; John Wiley: New York, 1985; p 443. (b) Adams, M. W. W.; Mortenson, L. E. *Ibid.*, p 519.

(3) (a) Cramer, S. P. *Adv. Inorg. Bioinorg. Mech.* **1983**, *2*, 259. (b) Cramer, S. P.; Wahl, R. C.; Rajagopalan, K. V. *J. Am. Chem. Soc.* **1981**, *103*, 7721. (c) George, G. N.; Bray, R. C.; Cramer, S. P. *Biochem. Soc. Trans.* **1986**, *14*, 651. (d) Bray, R. C.; George, G. N. *Ibid.* **1985**, *13*, 560. (e) Bray, R. C.; Gutteridge, S.; Storter, D. A.; Tanner, S. J. *Biochem. J.* **1979**, *177*, 357.

(4) Johnson, J. L.; Hainline, B. E.; Rajagopalan, K. V.; Arison, B. H. *J. Biol. Chem.* **1984**, *259*, 5414. Hawkes, T. R.; Bray, R. C. *Biochem. J.* **1984**, *219*, 481.

0002-7863/87/1509-5655$01.50/0 

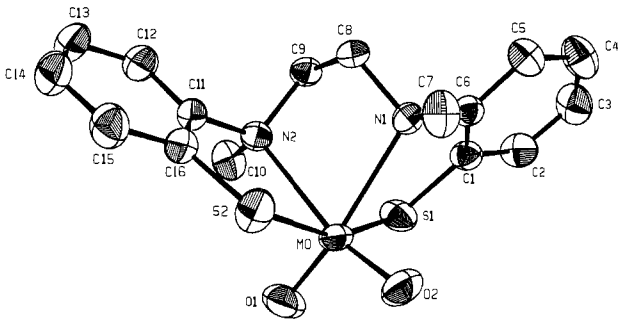


**Figure 1.** X-ray structure of $MoO_2L$. H atoms omitted for clarity.

trogen, or thioether ligands may also be present.[3]

One-electron reduction of these enzymes generates EPR active Mo(V) centers, which, omitting the SR ligands, have been formulated as $Mo^VO_2$ and $Mo^VO(OH)$ for the respective high- and low-pH forms of SO[3,5] and NR[2b,3a] from *E. coli*, and $Mo^VO(S)$ and $Mo^V(O)(SH)$ for the "very rapid"[3d] and "rapid"[3a,b] signals of XO, respectively. For the low-pH forms of reduced SO[6a,b] and NR[5,6c,d,7] and the reduced forms of XO[6a] superhyperfine coupling (0.9–1.6 mT) of an exchangeable $^1H$ has been observed, attributed to the OH or SH proton. Superhyperfine coupling of $^{17}O$ to the Mo(V) EPR signal, obtained by exchange with $H_2{}^{17}O$, has also been observed for SO[8] and XO.[8] Ligand oxo, OH, $H_2O$, and OR (R from substrate) are possible sources of the $^{17}O$ coupling. Additional couplings of other isotopes ($^{13}C$, $^{19}F$, $^{33}S$, e.g.) have also been reported under suitable conditions.[6a,9]

The other oxidation state implicated in turnover of these enzymes is Mo(IV). A single oxo group has been detected by EXAFS in each of the enzymes for this state.[3a-c]

Recently, coupling of an OH proton to the Mo(V) EPR signal of the one-electron reduced product of $MoO_2[S(CH_2)_2N(CH_3)(CH_2)_2N(CH_3)(CH_2)_2S]$ and of OH and SH proton couplings in related complexes with tetradentate $N_2O_2$ ligands have been observed in our laboratories.[10,11]

We report here the synthesis, X-ray structure, and electrochemical properties of $Mo^{VI}O_2L$ ($LH_2$ = *N,N'*-dimethyl-*N,N'*-bis(2-mercaptophenyl)ethylenediamine) and the EPR spectra of various oxo–Mo(V) complexes generated by one-electron reduction of $MoO_2L$ in solution under a variety of conditions. These spectra are consistent with the presence of $[MoO_2L]^-$, *cis*-MoO(OH)L, $[MoOSL]^-$, and *cis*-MoO(SH)L. The synthesis and properties of $Mo^VOClL$ are also described. The relevance of the results to the structures of the Mo(VI/V) centers in the enzymes is discussed.

## Results

Previous work by one of us has shown that one-electron electrochemical reduction of $Mo^{VI}O_2$ complexes with tetradentate $N_2O_2$ or $N_2S_2$ ligands having secondary amino groups results in deprotonation of the amino groups and loss of an oxo ligand as $H_2O$. Anionic $Mo^VO$ complexes result with the trans position empty or occupied by solvent.[12] This biomimetically undesirable result has been circumvented by synthesis of the tetradentate $N_2S_2$ ligand, *N,N'*-dimethyl-*N,N'*-bis(2-mercaptophenyl)ethylenediamine, and its $Mo^{VI}O_2$ complex.

**Table I.** Selected Bond Distances[a] and Bond Angles for $MoO_2L$

| atom 1 | atom 2 | bond distance, Å | atom 1 | atom 2 | atom 3 | bond angle, deg |
|---|---|---|---|---|---|---|
| Mo | S1 | 2.413 (1) | S1 | Mo | S2 | 159.91 (2) |
| Mo | S2 | 2.414 (1) | S1 | Mo | O1 | 88.92 (7) |
| Mo | O1 | 1.697 (2) | S1 | Mo | O2 | 103.04 (7) |
| Mo | O2 | 1.697 (2) | S1 | Mo | N2 | 85.63 (4) |
| Mo | N2 | 2.441 (2) | S1 | Mo | N1 | 77.06 (4) |
| Mo | N1 | 2.460 (2) | S2 | Mo | O1 | 102.39 (7) |
| | | | S2 | Mo | O2 | 89.50 (7) |
| | | | S2 | Mo | N2 | 77.45 (4) |
| | | | S2 | Mo | N1 | 87.94 (4) |
| | | | O1 | Mo | O2 | 107.4 (1) |
| | | | O1 | Mo | N2 | 92.45 (8) |
| | | | O1 | Mo | N1 | 161.38 (8) |
| | | | O2 | Mo | N2 | 158.27 (8) |
| | | | O2 | Mo | N1 | 87.89 (8) |
| | | | N2 | Mo | N1 | 74.52 (5) |

[a] Numbers in parentheses are estimated standard deviations in the last digits.

**Table II.** Electrochemical Parameters

| complex | $E_{1/2}$ (V vs. SCE) | $n$ ($e^-$/molecule)[g] |
|---|---|---|
| $MoO_2L$ | −1.06[a] | 1.00 |
| | −0.98[b] | 1.00 |
| | −0.94[c] | |
| | −0.97[d] | |
| $MoO_2L + 2H^+$ | −0.78[d,e] | |
| MoOClL | −0.46[f] | 1.00 |

[a] DMF, 0.10 M $[n\text{-}Bu_4N][BF_4]$, Pt. [b] MeCN, 0.10 M $[n\text{-}Bu_4N][BF_4]$, Pt. [c] THF, 0.10 M $[n\text{-}Bu_4N][BF_4]$, Pt. [d] DMF, 0.10 M $[n\text{-}Bu_4N][ClO_4]$, Hg. [e] Irreversible. [f] MeCN, 0.10 M $[Et_4N]Cl$, Pt. [g] Coulometric reduction.

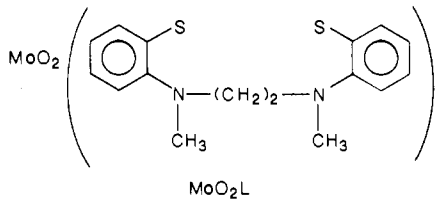


$MoO_2L$

**X-ray Structure of $MoO_2L$.** The X-ray crystal structure of $MoO_2L$ has been determined. It has distorted octahedral geometry with approximate $C_2$ symmetry (Figure 1), typical for $MoO_2(N_2S_2)$ complexes.[13] The two oxo groups are cis to one another and to the two thiolate groups of the tetradentate ligand L. The two tertiary amine atoms of L are cis to one another and approximately trans to the terminal oxo groups. The N–Mo–N angle, 74.52 (5)°, is more acute than similar angles in $MoO_2(N,S)_2$ compounds with bidentate chelating ligands,[13,14] presumably a result of the steric restrictions of the ethylenediamine backbone of L.

Table I summarizes the distances and angles of $MoO_2L$. It is interesting to compare the parameters for $MoO_2L$ with those of the corresponding complex with secondary amine atoms (L = $S_2(NH)_2$).[15] For the complex with the N–Me ligand, the O–

(5) Bray, R. C. *Adv. Enzymol. Rel. Areas Mol. Biol.* **1980**, *51*, 107.
(6) (a) Bray, R. C. In *Biological Magnetic Resonance*; Berliner, L. J., Reuben, J., Eds.; Plenum Press: New York, 1980; Vol. 2, p 45. (b) Bray, R. C.; Gutteridge, S.; Lamy, M. T.; Wilkinson, T. *Biochem. J.* **1983**, *211*, 227. (c) Gutteridge, S.; Bray, R. C.; Nottom, B. A.; Fido, R. J.; Hewitt, E. J. *Biochem. J.* **1983**, *213*, 137. (d) Vincent, S. P. Bray, R. C. *Biochem. J.* **1978**, *171*, 639.
(7) Solomonson, L. P.; Barber, M. J.; Howard, W. D.; Johnson, J. L.; Rajagopalan, K. V. *J. Biol. Chem.* **1984**, *259*, 849.
(8) (a) Bray, R. C.; Gutteridge, S. *Biochemistry* **1982**, *21*, 5992. (b) Gutteridge, S.; Malthouse, S. P. G.; Bray, R. C. *J. Inorg. Biochem.* **1979**, *11*, 355. (c) Morpeth, F. F.; George, G. N.; Bray, R. C. *Biochem. J.* **1984**, *220*, 235. Anisotropic coupling with $\langle A(^{17}O)\rangle$ of 0.68 mT is also observed with formamide as substrate.
(9) Wahl, R. C.; Rajagopalan, K. V. *J. Biol. Chem.* **1982**, *257*, 1354.
(10) Farchione, F.; Hanson, G. R.; Rodrigues, C. G.; Bailey, T. D.; Bagchi, R. N.; Bond, A. M.; Pilbrow, J. R.; Wedd, A. G. *J. Am. Chem. Soc.* **1986**, *108*, 831.
(11) Hinshaw, C. J.; Spence, J. T. *Inorg. Chim. Acta* **1986**, *125*, L17.
(12) Subramanian, P.; Spence, J. T.; Ortega, R. B.; Enemark, J. H. *Inorg. Chem.* **1984**, *23*, 2564. Rajan, O. R.; Spence, J. T.; Leman, C.; Minelli, M.; Sato, M.; Enemark, J. H.; Kroneck, P. M. H.; Sulger, K. *Inorg. Chem.* **1983**, *22*, 3065.
(13) Garner, C. D.; Bristow, S. In *Molybdenum Enzymes*; Spiro, T. G., Ed.; John Wiley: New York, 1985; p 343.
(14) Buchanan, I.; Minelli, M.; Ashby, M. T.; King, T. J.; Enemark, J. H.; Garner, G. D. *Inorg. Chem.* **1984**, *23*, 495.
(15) Bruce, A.; Corbin, J. L.; Dahlstrom, P. L.; Hyde, J. R.; Minelli, M.; Stiefel, E. I.; Spence, J. T.; Zubieta, J. *Inorg. Chem.* **1982**, *21*, 917.

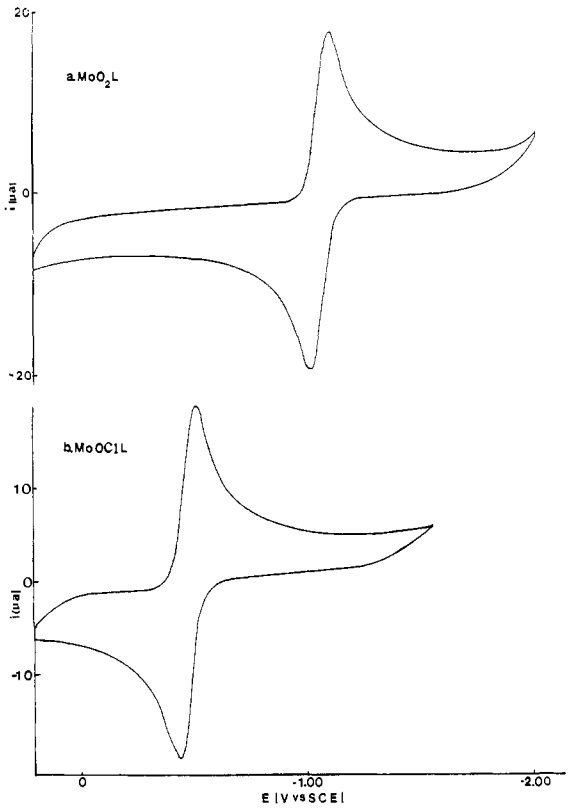


**Figure 2.** Cyclic voltammograms: (a) $MoO_2L$, $5.81 \times 10^{-4}$ M, DMF, 0.10 M $[n\text{-}Bu_4N][BF_4]$, Pt; (b) *trans*-MoOClL, $6.39 \times 10^{-4}$ M, MeCN, 0.10 M $[Et_4N]Cl$, glassy carbon. Scan rate = 0.100 V $s^{-1}$.

**Table III.** EPR Parameters for Analogue Complexes[a]

| complex | parameter | 1 | 2 | 3 | av | |
|---|---|---|---|---|---|---|
| $[MoO_2L]^-$ *c* | *g* | 1.9855 | 1.9121 | 1.8112 | 1.9007 | |
| | *A* ($^{95,97}$Mo) | 2.95 | 3.55 | 8.35 | *b* | b |
| $[MoOL]^+$ | *g* | 2.0020 | 1.9560 | 1.9445 | 1.9670 | |
| | *A* ($^{95,97}$Mo) | | | | 4.10 | |
| *cis*-MoO(OH)L | *g* | 1.9805 | 1.9470 | 1.9440 | 1.9570 | |
| | *A* ($^{95,97}$Mo) | | | | 4.40 | |
| | *A* ($^{1}$H) | 1.50 | 1.15 | 2.20 | 1.65 | |
| | *A* ($^{17}$O)[h] | | | | 0.82 | |
| | | | | | 0.25 | |
| $[MoOSL]^-$ *c* | *g* | 2.0165 | 1.9330 | 1.8885 | 1.9435 | |
| | *A* ($^{95,97}$Mo) | 5.00 | 2.65 | 4.40 | 4.10 | |
| | *A* ($^{17}$O)[h] | 0.20 | 0.35 | 0.75 | *b* | |
| *cis*-MoO(SH)L | *g* | 2.0160 | 1.9610 | 1.9535 | 1.9765 | |
| | *A* ($^{95,97}$Mo) | | | | 3.80 | |
| | *A* ($^{1}$H) | 0.90 | 1.10 | 1.05 | 1.05 | |
| | *A* ($^{17}$O)[h] | | | | 0.22 | |
| *trans*-MoOClL[d] | *g* | 2.0030 | 1.9530 | 1.9425 | 1.9700 | |
| | *A* ($^{95,97}$Mo) | 6.30 | 3.30 | 2.70 | 4.05 | |
| *trans*-MoO(OH)L[e] | *g* | 1.9820 | 1.9525 | 1.9415 | 1.9565 | |
| | *A* ($^{95,97}$Mo) | 6.70 | 3.40 | 2.45 | 4.20 | |
| *trans*-MoOFL[f] | *g* | 2.0030 | 1.9575 | 1.9450 | 1.9685 | |
| | *A* ($^{95,97}$Mo) | 6.40 | 4.15 | 2.00 | 4.20 | |
| *trans*-MoO(SH)L | *g* | 2.0195 | 1.9610 | 1.9545 | 1.9785 | |
| | *A* ($^{95,97}$Mo) | | | | 3.60 | |
| $[MoO(SPh)_4]^-$ *g* | *g* | 2.017 | 1.979 | 1.979 | 1.990 | |
| | *A* ($^{95,97}$Mo) | 5.23 | 2.23 | 2.23 | 3.23 | |
| | *A* ($^{17}$O) | 0.068 | 0.310 | 0.310 | 0.228 | |

[a] Anisotropic spectra measured in frozen MeCN, DMF, or THF, 0.10 M $[n\text{-}Bu_4N][BF_4]$; isotropic spectra in MeCN, DMF, or THF, 0.10 M $[n\text{-}Bu_4N][BF_4]$; anisotropic *g* and *A* values and ($A(^{17}O)$) from computer simulation; precision of $g = \pm 0.0005$, precision of $A = \pm 0.05$; *A* values are in mT. [b] (*A*) impossible to obtain because of line width. [c] *g* and *A* tensors in all planes coincident. [d] $\alpha_{12} = 17°$ ($\alpha_{12}$ = noncoincidence angle between *g* and *A* tensors in plane containing $g_1$ and $g_2$). [e] $\alpha_{12} = 27°$. [f] $\alpha_{12} = 12°$. [g] References 10 and 21.

Mo–O bond angle is smaller (107.4 (1)° vs. 109.9 (1)°), the S–Mo–S bond angle larger (159.91 (2)° vs. 156.5 (1)°), and the average Mo–N bond length longer (2.450 (2) Å vs. 2.368 (3) Å),

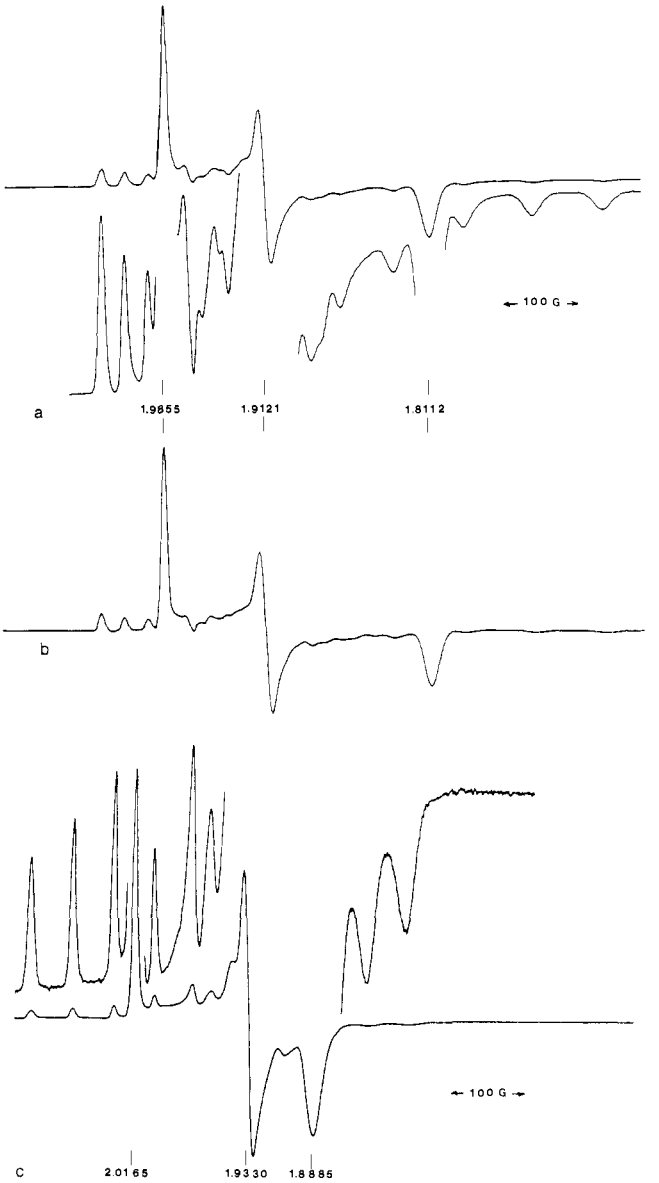


**Figure 3.** EPR spectra, 77 K: (a) $[MoO_2L]^-$, $2.00 \times 10^{-3}$ M, DMF; (b) simulation of spectrum a; (c) $[MoOSL]^-$, $5.00 \times 10^{-2}$ M, MeCN.

most likely a result of a steric effect of the N–Me groups. The same result is found when comparing tetradentate $N_2O_2$ complexes (L = $O_2(N\text{–}Me)_2$; L = $O_2(NH)_2$) with otherwise similar ligands.[12,16] The Mo–thiolate sulfur bond distances in $MoO_2L$ differ very little, however, from those for L = $S_2(NH)_2$ and are almost the same as those found for the closely related $S_4$ tetradentate complex (L = $S_4$, 2 thiolate S and 2 thioether S atoms).[17]

**Electrochemistry of $MoO_2L$.** $MoO_2L$ undergoes reversible one-electron electrochemical reduction in MeCN, DMF, and THF at all temperatures used, on the time scales of both cyclic voltammetry and coulometry (Figure 2a, Table II). The cyclic voltammogram (CV) of the reduced product, when scanned in the anodic direction, is identical with that of $MoO_2L$, indicating that the reduced species is stable under the conditions used. Coulometric reoxidation of the reduced species at room temperature facilely removes one electron, giving the original complex without detectable loss. No additional reduction processes are observed in the CV to −2.00 V vs. SCE in any solvent. The CV of $MoO_2L$ in MeCN at room temperature in the presence of excess

(16) Spence, J. T.; Hinshaw, C. C.; Enemark, J. H.; Merbs, S. L.; Ortega, R. B. In *Frontiers in Bioinorganic Chemistry*; Xavier, A. V., Ed.; VCH Verlagsgesellschaft: Weinheim, **1986**; p 54.
(17) Kaul, B. B.; Enemark, J. H.; Merbs, S. L.; Spence, J. T. *J. Am. Chem. Soc.* **1985**, *107*, 2885.

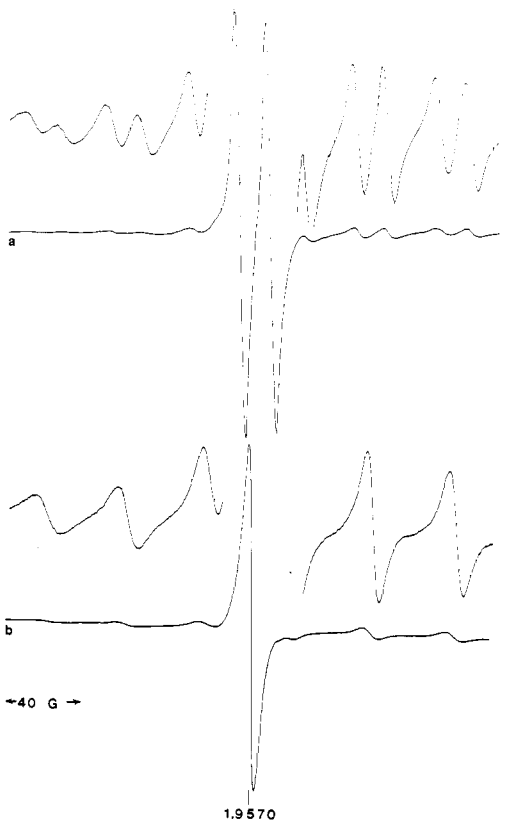


**Figure 4.** EPR spectra, −42 °C, THF, 0.10 M [*n*-$Bu_4N$][$BF_4$]: (a) *cis*-MoO(OH)L, 1.5 M $H_2O$; (b) *cis*-MoO($O^2H$)L, 1.5 M $^2H_2O$.

$CF_3COOH$ at a HMD electrode shows an irreversible reduction peak at a more positive potential, and no oxidation peak in the potential range available on Hg (Table II).

**EPR of Reduced $MoO_2L$.** One-electron reduction of $MoO_2L$ at a Pt cathode in MeCN, DMF, or THF at room temperature gives a ~100% monomeric Mo(V) product having an unusual rhombic, highly anisotropic frozen EPR spectrum at X-band frequency with exceptionally small $g$ and large $A$ values (particularly $g_3$ and $A_3$, Figure 3a, Table III). The room temperature X-band EPR spectrum is broad (~7.5 mT), presumably as a result of incomplete rotational averaging, while $\langle g \rangle$ (1.9007) is the lowest value reported for any Mo(V) complex containing thiolate ligands.[11,18] Addition of trace amounts of $O_2$ to the reduced solution results in partial reoxidation of the Mo(V) species with generation of superoxide radical ($O_2^-$), detected by EPR. Reaction of the reduced complex with $CF_3COOH$ at room temperature gives a new deep purple species having an EPR spectrum ($\langle g \rangle$ = 1.9670) typical of $Mo^VO$ complexes,[18] with no evidence of $^1H$ coupling to Mo(V). In the presence of 1.5 M $H_2O$ at room temperature, a small amount of the $\langle g \rangle$ = 1.9670 species in addition to the $\langle g \rangle$ = 1.9007 species is obtained. The same reaction at room temperature in the presence of [$Et_4N$]Cl gives a Mo(V) species having an EPR spectrum identical with that of MoOClL ($\langle g \rangle$ = 1.9700) (vide infra).

One-electron reduction of $MoO_2L$ in wet (1.5 M $H_2O$) THF at −42 °C in a specially designed cell in the EPR cavity generates a species with a solution EPR spectrum ($\langle g \rangle$ = 1.9570) typical of oxo–Mo(V) complexes,[18] except that both the $I = 0$ and $^5/_2$ features of the spectrum are split into doublets (Figure 4a). Generation of the signal in the presence of 1.5 M $^2H_2O$ results in collapse of the doublets in the spectrum, indicating that the superhyperfine coupling (1.65 mT, Table III) arises from a single proton in the reduced complex (Figure 4b). The frozen spectrum

(18) Scullane, M. I.; Taylor, R. D.; Minelli, M.; Spence, J. T.; Yamanouchi, K.; Enemark, J. H.; Chasteen, N. D. *Inorg. Chem.* **1979**, *18*, 3213. Cleland, W. E., Jr.; Barnhart, K. M.; Yamanouchi, K.; Collinson, D.; Mabbs, F. E.; Ortega, R. B.; Enemark, J. H., in press.

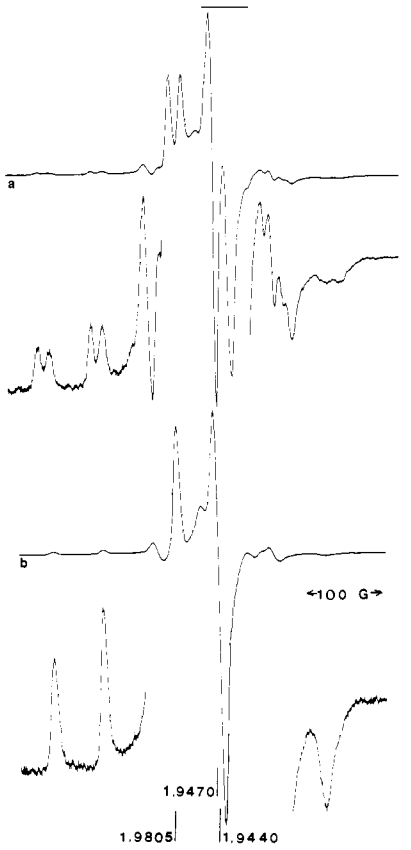


**Figure 5.** EPR spectra, −135 °C, THF, 0.10 M [*n*-$Bu_4N$)[$BF_4$]: (a) *cis*-MoO(OH)L, 1.5 M $H_2O$; (b) *cis*-MoO($O^2H$)L, 1.5 M $^2H_2O$.

exhibits $^1H$ coupling to all three components of the $g$ tensors (Figure 5a); the doublets in the frozen spectrum also collapse when the signal is generated in the presence of 1.5 M $^2H_2O$ (Figure 5b). Warming to room temperature results in loss of the doublet species and the appearance of other peaks in the spectrum.

Reduction of $MoO_2L$ in THF at −42 °C in the presence of excess [$Et_4N$][OH] or excess [$Et_4N$]F generates a broad solution EPR spectrum ($\langle g \rangle$ = 1.9007) identical with that obtained by reduction of $MoO_2L$ at room temperature in MeCN.

Addition of excess [*n*-$Bu_4N$]SH in THF or MeCN at room temperature to $MoO_2L$ reduces it to a Mo(V) species having a broad room temperature EPR spectrum, similar to that obtained by electrochemical reduction of $MoO_2L$ in MeCN at room temperature, but with smaller line width (~3.0 mT) and higher $\langle g \rangle$ (1.9435) and lower $\langle A \rangle$ values; the frozen spectrum (Figure 3c) is also quite similar to that obtained by electrochemical reduction of $MoO_2L$ in MeCN, but with less anisotropy (particularly in $g_3$). Addition of $CF_3COOH$ to the reduced solution at −78 °C gives a solution EPR signal similar to that obtained upon electrochemical reduction of $MoO_2L$ in wet THF at −42 °C, but with higher $\langle g \rangle$ (1.9765) and lower $\langle A \rangle$ and also exhibiting doublets in the $I$ = 0 and $^5/_2$ features (Figure 6a). The frozen EPR spectrum is rhombic, with doublets observed in all three $g$ tensors (Figure 7a). Similar treatment of the solution with $CF_3COO^2H$ in $^2H_2O$ results in collapse of the doublets, again indicating superhyperfine coupling of a single proton to Mo(V) (Figures 6b and 7b). As the temperature is raised above ca. −60 °C, the doublet signal disappears, and another EPR signal ($\langle g \rangle$ = 1.9785) appears. Addition of $CF_3COOH$ to the reduced solution at room temperature in THF gives a transient doublet EPR signal identical with the stable signal obtained at −78 °C. This transient signal changes rapidly (5–10 min) to the $\langle g \rangle$ = 1.9785 signal.

To facilitate measurement of $^{17}O$ superhyperfine coupling constants, $MoO_2L$ was isotope substituted with $^{17}O$ ($I = {}^5/_2$; 50% atom %) and/or $^{98}Mo$ ($I$ = 0, 96 atom %). Reduction of $Mo^{17}O_2L$ at room temperature in MeCN gives no evidence for $^{17}O$ superhyperfine coupling in the solution EPR spectrum because of the line width of the signal. The frozen spectrum, however, is

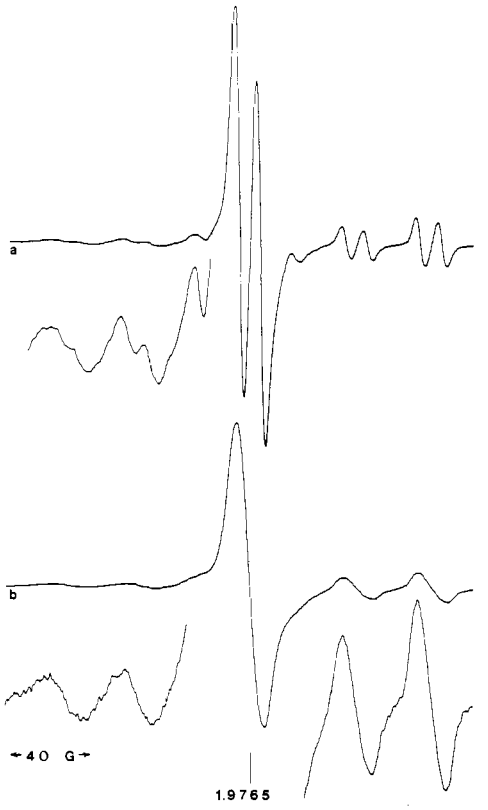


**Figure 6.** EPR spectra, −78 °C, 1.00 × $10^{-3}$ M, THF, 0.10 M [*n*-$Bu_4N$][$BF_4$]: (a) *cis*-MoO(SH)L; (b) *cis*-MoO($S^2H$)L.

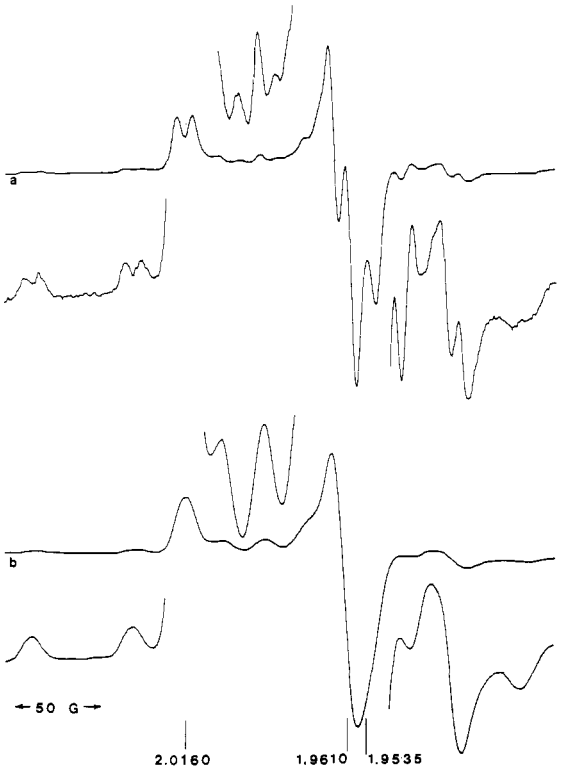


**Figure 7.** EPR spectra, −135 °C, 1.00 × $10^{-3}$ M, THF, 0.10 M [*n*-$Bu_4N$][$BF_4$]: (a) *cis*-MoO(SH)L; (b) *cis*-MoO($S^2H$)L.

broadened significantly in all three *g* features (Figure 8b).

Reduction of $^{98}Mo^{17}O_2L$ in wet THF at −42 °C gives a solution EPR spectrum exhibiting the effects of $^{17}O$ ($I = {}^5/_2$) superhyperfine coupling to Mo(V), but with the $^{95,97}Mo$ hyperfine features eliminated. The coupling is evident in the $I = 0$ doublet (also split by $^1H$) as broadening of the main peaks, and the presence of additional shoulders and peaks, when compared with the spectrum

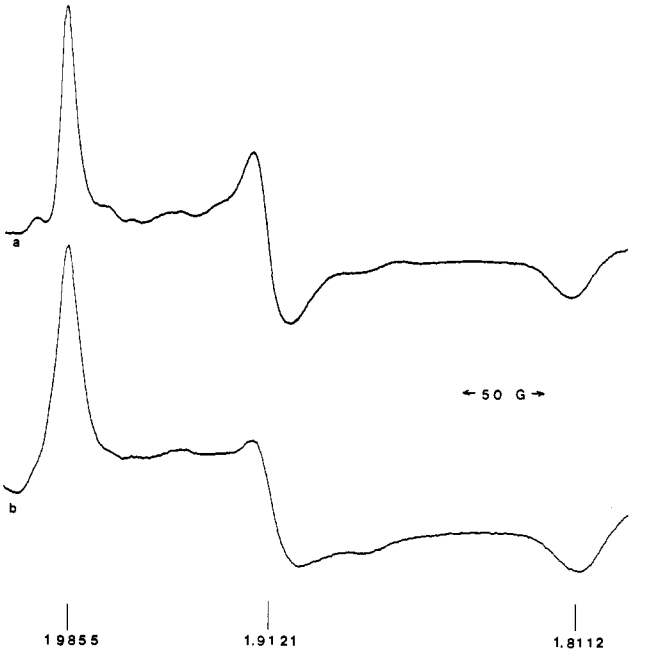


**Figure 8.** EPR spectra, 77 K, 1.00 × $10^{-2}$ M, MeCN, 0.10 M [*n*-$Bu_4N$][$BF_4$]: (a) $[MoO_2L]^-$; (b) $[Mo^{17}O_2L]^-$.

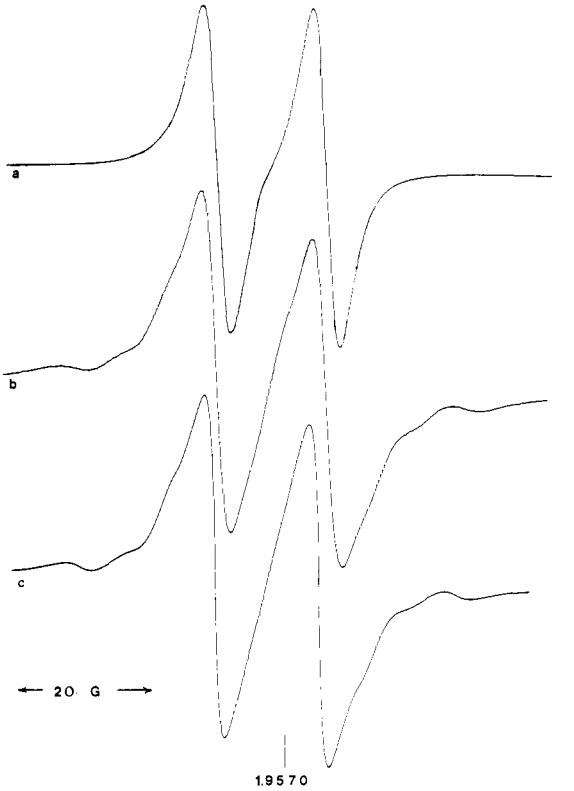


**Figure 9.** EPR spectra, −42 °C, THF, 0.10 M [*n*-$Bu_4N$][$BF_4$], 1.5 M $H_2O$: (a) *cis*-$^{98}$MoO(OH)L; (b) *cis*-$^{98}Mo^{17}O(^{17}OH)$L; (c) simulation of spectrum b, $^{17}O$ ($A$) = 0.25, 0.82 mT.

of reduced $^{98}Mo^{16}O_2L$ (Figure 9a,b). Computer simulation with coupling of two nonequivalent $^{17}O$ nuclei of 0.82 and 0.25 mT (Table III) gave a good fit to the experimental spectrum (Figure 9c) while simulations with only one $^{17}O$ with coupling of 0.82 and 0.25 mT were unsatisfactory (Figure 10). The effects of $^{17}O$ coupling on the frozen spectrum are difficult to discern at X-band frequencies. Multifrequency EPR experiments, currently underway, are required to obtain the anisotropic $^{17}O$ coupling constants.

Reduction of $Mo^{17}O_2L$ with excess [*n*-$Bu_4N$]SH gives a solution EPR spectrum with no evidence for $^{17}O$ superhyperfine coupling,

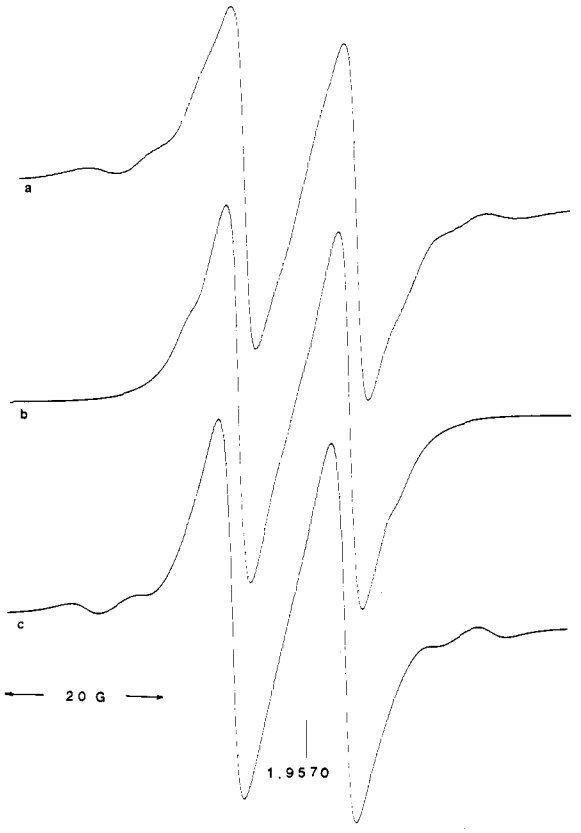


**Figure 10.** EPR spectra, −42 °C, THF, 0.10 M [$n$-$Bu_4N$][$BF_4$], 1.5 M $H_2O$: (a) *cis*-$^{98}Mo^{17}O(^{17}OH)L$; (b) simulation of spectrum a, *cis*-$^{98}Mo^{17}O(OH)L$, $^{17}O$ ($A$) = 0.25 mT; (c) simulation of spectrum a, *cis*-$^{98}MoO(^{17}OH)L$, $^{17}O$ ($A$) = 0.82 mT.

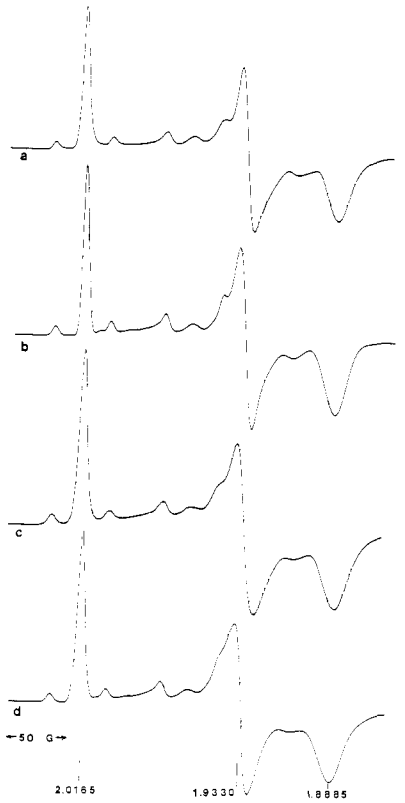


**Figure 11.** EPR spectra, 77 K, 5.00 × $10^{-2}$ M, THF: (a) [MoOSL]$^-$; (b) simulation of spectrum a; (c) [$Mo^{17}OSL$]$^-$; (d) simulation of spectrum c.

again because of the line width of the signal. The frozen spectrum, however, exhibits small but definite line broadening in all three

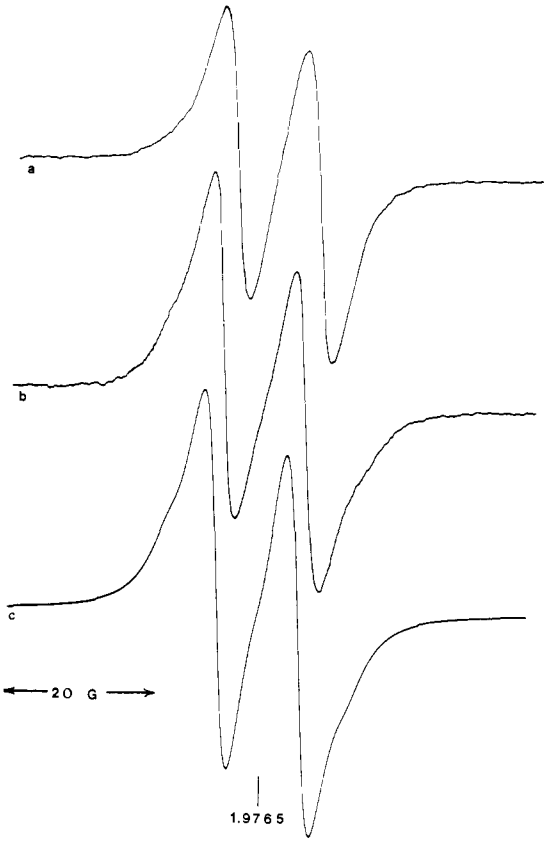


**Figure 12.** EPR spectra, −78 °C. 1.00 × $10^{-3}$ M, THF, 0.10 M [$n$-$Bu_4N$][$BF_4$]: (a) *cis*-$^{98}MoO(SH)L$; (b) *cis*-$^{98}Mo^{17}O(SH)L$; (c) simulation of spectrum b.

$g$ features of Figure 11c. The effect is most evident at $g_2$ (Table III, Figure 11). The $^{17}O$ coupling is small ($\langle A(^{17}O)\rangle \cong 0.4$ mT), and estimates of the anisotropic $^{17}O$ coupling constants could be obtained by computer simulation with a single coupled $^{17}O$ (Table III).

Addition of $CF_3COOH/H_2O$ at −78 °C to solutions generated from $^{98}Mo^{17}O_2L$ with [$n$-$Bu_4N$]SH gives a solution EPR spectrum exhibiting the effects of $^{17}O$ coupling (Figure 12b, Table III). Computer simulation with coupling of a single $^{17}O$ of 0.22 mT gave a satisfactory fit to the experimental spectrum (Figure 12c). Determination of the anisotropic $^{17}O$ coupling constants will require multifrequency experiments.

**MoOClL.** This deep blue-green complex was prepared from $(NH_4)_2MoOCl_5$ and the ligand. Attempts to grow crystals suitable for X-ray crystallography were unsuccessful. The CV of the complex exhibits a reversible one-electron reduction process at −0.46 V vs. SCE in MeCN or DMF in the presence of [$Et_4N$]Cl (Figure 2b, Table II). With [$n$-$Bu_4N$][$BF_4$] as electrolyte MoOClL undergoes an irreversible reduction at the same potential which is coupled to an oxidation at −0.015 V vs. SCE in the CV. Coulometric reduction in the presence of [$Et_4N$]Cl by one electron, however, results in decomposition, giving a CV without the −0.46 V couple and exhibiting several new small peaks, indicating the initial Mo(IV) complex observed in the CV under these conditions is unstable on the coulometric time scale.

MoOClL is stable in solution (MeCN, DMF, THF) and is ~100% monomeric. The EPR signal ($\langle g\rangle$ = 1.9700) is as expected for an oxo–Mo(V) complex with two thiolate ligands.[18] Addition of excess [$n$-$Bu_4N$]OH or [$n$-$Bu_4N$]F in MeCN gives EPR signals having different $g$ values and colors, but with no detectable $^1H$ or $^{19}F$ superhyperfine coupling to Mo(V). Addition of 1.5 equiv of [$n$-$Bu_4N$]SH gives the same EPR signal ($\langle g\rangle$ = 1.9785) observed upon room temperature protonation of the species obtained by reduction of $MoO_2L$ with excess [$n$-$Bu_4N$]SH (vide supra), while addition of excess [$n$-$Bu_4N$]SH at room temperature gives the same EPR signal ($\langle g\rangle$ = 1.9435) observed upon addition of this reagent to $MoO_2L$.

## Discussion

The reversible one-electron reduction of $MoO_2L$ in MeCN at room temperature is highly unusual for dioxo–Mo(VI) complexes. These species generally exhibit irreversible reduction processes (as a result of loss of an oxo ligand) often coupled to the formation of binuclear species. On the basis of the reversible electrochemistry, the unusual EPR spectra, and the protonation and substitution reactions of the reduced species, the reduction product is most reasonably formulated as a stable dioxo–Mo(V) complex:

$$MoO_2L \underset{-e^-}{\overset{e^-}{\rightleftharpoons}} [MoO_2L]^-$$

Further evidence for this formulation is the observation of the formation of superoxide ($O_2^-$) and regeneration of $MoO_2L$ upon exposure of the reduced solution to traces of oxygen.[19]

$$[MoO_2L]^- + O_2 \rightarrow O_2^- + MoO_2L$$

The highly anisotropic EPR spectrum (Figure 3a) is a fingerprint for $[MoO_2L]^-$; its extreme anisotropy is mainly a result of a particularly low $g_3$, and it indicates a significant spin–orbit coupling effect. The interpretation of frozen EPR spectra of $Mo^VO$ species generally assumes $O_h$ or $C_{4v}$ symmetry with the $z$ axis along the Mo–oxo bond, and the unpaired electron in the $d_{xy}$ or $d_{x^2-y^2}$ orbital.[18] This is the first detailed report of a stable dioxo–Mo(V) complex, however, and neither the geometry nor the electronic structure is known.[10,11] The observation of significant line broadening in all $g$ features of the frozen EPR spectrum (Figure 8b) of $[Mo^{17}O_2L]^-$ indicates coupling to $^{17}O$ is present. Accurate determination of $^{17}O$ coupling constants by multifrequency EPR is underway and should provide additional structural information.

The X-ray structure of $MoO_2L$ does not suggest any reason why a $[Mo^VO_2L]^-$ complex, previously observed in only two cases,[10,11] is particularly stable with this ligand. Comparison of the structure with that of the corresponding complex with secondary amine atoms (NH) suggests a significant steric effect of the N–Me groups, resulting in compression of the O–Mo–O bond angle, lengthening of the Mo–N bonds, and, most likely, inhibition of the formation of binuclear Mo(V) species. A further aspect is that neither $MoO_2L$ nor $[MoO_2L]^-$ exchange oxygen with $H_2O$ on a time scale of hours. This is in marked contrast to the rapid exchange exhibited with several closely related $Mo^{VI}O_2$ species.[20] Interestingly, the latter exhibit irreversible electrochemistry.

Protonation of $[MoO_2L]^-$ with $CF_3COOH$ at room temperature in MeCN results in an EPR spectrum ($\langle g \rangle$ = 1.9670) typical of $Mo^VO$ complexes.[18] There is no evidence of $^1H$ superhyperfine coupling, suggesting that this species is either *trans*-MoO(OH)L or $[MoOL]^+$, the latter arising from protonation and loss of $H_2O$ from unstable *cis*-MoO(OH)L. The irreversible CV obtained for the room temperature reduction of $MoO_2L$ in the presence of $CF_3COOH$ at the HMD electrode indicates the reduced species undergoes a chemical change in addition to protonation. This and evidence from substitution reactions of MoOClL (vide infra) supports $[MoOL]^+$ as the correct formulation.

In wet THF at −42 °C, the observed reduction product ($\langle g \rangle$ = 1.9570) is protonated (Figure 4). The proton is strongly coupled (1.65 mT), and comparison with related systems[10,11] indicates the presence of *cis*-MoO(OH)L. Additional evidence for this formulation is the following: (i) reduction under these conditions in the presence of the strong bases $OH^-$ and $F^-$ gives the conjugate base $[MoO_2L]^-$; (ii) observation of superhyperfine coupling of two $^{17}O$ nuclei of 0.82 and 0.25 mT (Figure 9), consistent with the presence of both OH and oxo ligands. Coupling of 0.228 mT is observed for the axial oxo group in $[Mo^{17}O(SPh)_4]^-$,[10,21] in which the oxo ligand valence orbitals are orthogonal, to first order, to the magnetic orbital.

**Scheme I**

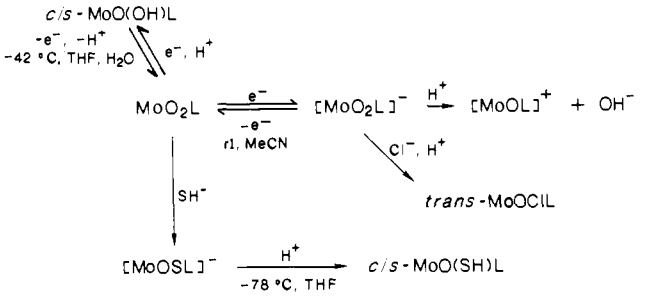


**Scheme II**

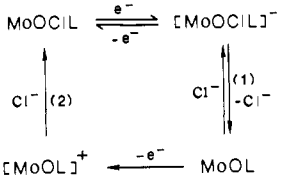


The highly anisotropic spectrum (Figure 3c) obtained upon reduction of $MoO_2L$ with excess $[n\text{-}Bu_4N]SH$ at room temperature strongly suggests the reduction product is $[MoO(S)L]^-$ or $[MoS_2L]^-$. The spectrum obtained upon reduction of $Mo^{17}O_2L$ (50 atom % $^{17}O$) under these conditions (Figure 11) is definitely broadened in all $g$ features (estimated anisotropic $^{17}O$ coupling constants are found in Table III), confirming the presence of $[MoOSL]^-$. Consequently the protonated species obtained at −78 °C (Figure 6) is either *cis*-MoS(OH)L or *cis*-MoO(SH)L. The latter formulation is supported by the following observations: (i) the $^{17}O$ coupling constant (0.22 mT) is almost identical with that observed for the oxo group in $[Mo^{17}O(SPh)_4]^-$ (0.228 mT)[10,21] and to the smaller $^{17}O$ constant (0.25 mT) observed in $Mo^{17}O(^{17}OH)L$, and much smaller than the larger $^{17}O$ constant (0.82 mT) in the latter complex; (ii) the $^1H$ coupling constant (1.05 mT) is significantly smaller than that for *cis*-MoO(OH)L (1.65 mT) and for the closely related *cis*-$MoO(OH)(S(CH_2)_2N(CH_3)(CH_2)_2N(CH_3)(CH_2)_2S)$ (1.50 mT);[10] and (iii) the observed $\langle g \rangle$, 1.9765, is much higher than that for *cis*-MoO(OH)L, 1.9570. Substitution of sulfide for oxo in *cis*-$MoOCl_2L'$ (L' = hydrotris(3,5-dimethylpyrazolyl)borate) to give *cis*-$MoSCl_2L'$ lowers $\langle g \rangle$ from 1.947 to 1.928.[22a] A decrease in $\langle g \rangle$ has also been observed when sulfide is substituted for oxo in $V^{IV}O$ complexes.[22b] A similar result would be expected if the protonated species is MoS(OH)L. These results are summarized in Scheme I.

The dependence of the cyclic voltammetry of MoOClL on the presence of $[Et_4N]Cl$ as electrolyte can be rationalized by Scheme II. With excess $Cl^-$ present, equilibrium 1 favors $[MoOClL]^-$ and reversible behavior is observed. In its absence, MoOL is favored, and oxidation follows the alternative route, indicating equilibrium 1 is slow, while reaction 2 is fast. One-electron coulometric reduction indicates MoOL is unstable, however, and decomposes to unknown products.

The EPR results from MoOClL indicate this is most likely the trans isomer, since reaction with $[n\text{-}Bu_4N]OH$, $[n\text{-}Bu_4]SH$, and $[n\text{-}Bu_4N]F$ gives species having EPR spectra with different colors and $g$ values, but without evidence of $^1H$ or $^{19}F$ coupling; such coupling would be expected for the cis isomers.[10,11] Since reaction of MoOClL with $[n\text{-}Bu_4N]OH$ gives a species with a significantly different $\langle g \rangle$ value (and color) from that obtained by protonation of $[MoO_2L]^-$ in MeCN at room temperature, the latter product is most likely the cation $[MoOL]^+$; protonation of $[MoO_2L]^-$ in

(19) Superoxide ion ($O_2^-$) is not observed in the oxidation of mono oxo–$Mo^V$ complexes by $O_2$; this may be a result of an oxidative addition reaction to form the $Mo^{VI}O_2$ complex and $H_2O_2$.

(20) Corbin, J. L.; Miller, K. F.; Pariyadath, N.; Wherland, S.; Bruce, A. E.; Stiefel, E. I. *Inorg. Chim. Acta* **1984**, *90*, 41.

(21) Hanson, G. R.; Brunette, A. A.; McDonnell, A. E.; Murray, K. S.; Wedd, A. G. *J. Am. Chem. Soc.* **1981**, *103*, 1953. Hanson, G. R.; Wilson, G. L.; Bailey, T. D.; Pilbrow, J. R.; Wedd. A. G., in press.

(22) (a) Young, C. G.; Collison, D.; Mabbs, F. E.; Enemark, J. H. *Inorg. Chem.*, in press. (b) Money, J. K.; Folting, K.; Huffman, J. C.; Collison, D.; Temperly, J.; Mabbs, F. E.; Christou, G. *Inorg. Chem.* **1986**, *25*, 4583. Callahan, K. P.; Durand, P. J. *Inorg. Chem.* **1980**, *19*, 3211.

**Table IV.** Selected EPR Parameters for Enzymes and Analogue Compounds

| center | g values | | | | $A(^1H)$,[a] mT | | | | $A(^{17}O)$, mT | | | |
|---|---|---|---|---|---|---|---|---|---|---|---|---|
| | $g_1$ | $g_2$ | $g_3$ | $\langle g \rangle$ | $A_1$ | $A_2$ | $A_3$ | $\langle A \rangle$ | $A_1$ | $A_2$ | $A_3$ | $\langle A \rangle$ |
| $[MoOSL]^-$ | 2.0165 | 1.9330 | 1.8885 | 1.9433 | | | | | 0.20 | 0.35 | 0.75 | 0.43 |
| XO (very rapid, xanthine)[c,d] | 2.0252 | 1.9550 | 1.9494 | 1.9765 | | | | | 1.34 | 1.40 | 1.36 | 1.37 |
| XO (very rapid, 2-amino-4-hydroxy-6-formylpteridine)[e] | 2.0221 | 1.9551 | 1.9466 | 1.9746 | | | | | | | | |
| XO (alloxanthine)[g] | 2.0279 | 1.9593 | 1.9442 | 1.9771 | | | | | | | | |
| MoO(SH)L | 2.0160 | 1.9610 | 1.9535 | 1.9765 | 0.90 | 1.10 | 1.05 | 1.05 | | | | 0.22 |
| XO (rapid type 1, xanthine)[c,g] | 1.9906 | 1.9707 | 1.9654 | 1.9756 | 1.20 | 1.30 | 1.30 | 1.27 | | | | 1.4 |
| XO (rapid type 2, xanthine)[c,g] | 1.9951 | 1.9712 | 1.9616 | 1.9760 | 1.07 | 0.98 | 0.93 | 1.01 | | | | 1[b] |
| MoO(OH)L | 1.9805 | 1.9470 | 1.9440 | 1.9570 | 1.50 | 1.15 | 2.20 | 1.65 | | | | 0.82, 0.25 |
| XO (slow, aquo)[c,g] | 1.9719 | 1.9671 | 1.9551 | 1.9647 | 1.66 | 1.66 | 1.56 | 1.63 | | | | 1[b] |
| SO (low pH, aquo)[c,g] | 2.0037 | 1.9720 | 1.965 (8) | 1.980 (5) | 0.85 | 0.80 | 1.30 | 0.98 | | | | 0.6 |
| SO (high pH)[c,g] | 1.9872 | 1.9641 | 1.9531 | 1.9681 | | | | | | | | 1.3 |
| NR (low pH, aquo, *E. coli*)[c] | 1.9989 | 1.9855 | 1.9628 | 1.9824 | 1.11 | 0.84 | 0.81 | 0.92 | | | | |
| NR (high pH, *E. coli*)[c] | 1.9870 | 1.9805 | 1.9612 | 1.9762 | | | | | | | | |
| NR (signal A, spinach)[h] | 1.9957 | 1.9692 | 1.9652 | 1.9767 | 1.20 | 1.25 | 1.45 | 1.30 | | | | |
| NR (low pH, *C. vulgaris*)[i] | 1.994 | 1.969 | 1.967 | 1.977 | 1.0 | 1.1 | 1.4 | 1.2 | | | | |

[a] Strongly coupled protons only. [b] Preliminary value for the most strongly coupled oxygen. See ref 8. [c] Reference 6a. [d] Reference 41. [e] Reference 42. [f] Reference 43. [g] Reference 8: $^{17}O$ data for XO rapid type 1 and type 2 were generated in the presence of purine and borate, respectively. [h] Reference 6c. [i] Reference 7.

the presence of $[Et_4N]Cl$ gives *trans*-MoOClL, as determined by EPR, consistent with this formulation.

The *trans*-MoO(X)L complexes (X = Cl, F, OH, SH) exhibit a wide range in $\langle g \rangle$ (1.9565–1.9785), indicating the trans ligand has considerable influence on $\langle g \rangle$, even though it is not in the $d_{xy}$ or $d_{x^2-y^2}$ plane. If these complexes have $C_s$ symmetry, the $g$ and $A$ tensors in the $y$ direction orthogonal to the mirror plane ($z$ direction along the oxo–Mo bond) must be coincident. Since the angle of noncoincidence for X = Cl, OH, and F complexes is in the $g_1$–$g_2$ plane, this means $g_2 = g_x$ and $g_3 = g_y$ ($g_x > g_y$). A similar case has been reported for *trans*-$MoOCl_3$(byp) and *trans*-$MoOCl_3$(phen), and analysis of their EPR spectra concluded the anisotropy in $g_x$ and $g_y$ is a result of mixing of the $d_{z^2}$ orbital into the ground state $d_{x^2-y^2}$ orbital.[18] This may account for the effect of different trans substituents on the $g$ values of MoO(X)L complexes.

### Relationship to Molybdenum Hydroxylases and Related Enzymes

EPR data for the molybdenum hydroxylases have been interpreted[2,3,5,6] in terms of $Mo^VO_2$, $Mo^VO(OH)$, $Mo^VOS$, and $Mo^VO(SH)$ centers. The present work provides strong evidence for the existence of such centers in model complexes with the ligand L.

The "rapid" and "slow" EPR signals of XO are generated from functional and nonfunctional (desulfo) enzyme, respectively. The $g$ values of these signals are compared with those of *cis*-MoO(SH)L and *cis*-MoO(OH)L in Figure 13 and Table IV. The value of $\langle g \rangle$ is higher for MoO(SH)L than for MoO(OH)L, as is the case for the rapid signal relative to the slow signal, consistent with substitution of a sulfur ligand for an oxygen ligand. The value of $\langle g \rangle$ for *cis*-MoO(SH)L is the same as that of the rapid signal, while that of *cis*-MoO(OH)L is somewhat smaller than that of the slow signal.

The absolute magnitudes of anisotropy of the $g$ values are greater for both analogue complexes than for the corresponding enzyme signals (Figure 13a); the anisotropy of the rapid signal is greater than that of the slow signal, however, and this is also true for *cis*-MoO(SH)L vs. *cis*-MoO(OH)L.

The average superhyperfine coupling constant $\langle A(^1H) \rangle$ for the strongly coupled $^1H$ of the rapid signal, 1.27 mT, is quite similar to that of MoO(SH)L, 1.05 mT, and the anisotropies are both <0.2 mT. $\langle A(^1H) \rangle$ for the slow signal is higher (1.63 mT) and this is mirrored by MoO(OH)L (1.65 mT), but the anisotropy of the slow signal is smaller than that of MoO(OH)L.

This comparison of the $g$ and $A(^1H)$ values is consistent with $Mo^VO(SH)$ and $Mo^VO(OH)$ centers being responsible for the rapid and slow signals of XO.

Detailed comparison of $^{17}O$ superhyperfine coupling constants is not possible as anisotropic data for all of the enzyme and

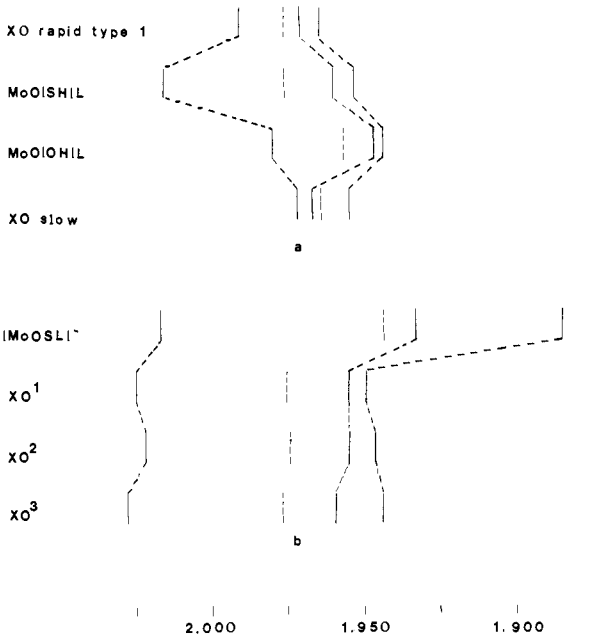


**Figure 13.** Comparison of $g$ values for xanthine oxidase and analgoues: (a) rapid and slow signals; (b) Very rapid signals—(1) xanthine as substrate; (2) 2-amino-4-hydroxy-6-formylpteridine as substrate; (3) alloxanthine as inhibitor. Dashed vertical lines are $\langle g \rangle$.

analogue species are not yet available. A single $^{17}O$ coupling ($A(^{17}O)$) of 1.4 mT is observed for the rapid type 1 signal generated from purine for XO.[8] This can be compared to 0.228 mT for the oxo group in $[Mo^{17}O(SPh)_4]^-$,[21] 0.25 mT (assigned to the oxo group, this work) in $Mo^{17}O(^{17}OH)L$, and 0.22 mT for the oxo group in $Mo^{17}O(SH)L$ (this work). Bound product (OR) rather than an oxo ligand, at a $Mo^VO(SH)(^{17}OR)$ center, is clearly a plausible source of the coupling in the enzyme.

The slow signal for XO exhibits coupling to more than one oxygen atom,[8] with $\langle A(^{17}O) \rangle$ of 1 mT estimated for the more strongly coupled oxygen (Table IV). A value of 0.82 mT has been assigned to the OH ligand of MoO(OH)L (this work). An OH ligand is suggested as the source of this coupling in the slow signal, although a substrate (OR) oxygen remains a possibility.

Functional XO exhibits another EPR signal, the "very rapid", which appears prior to development of the rapid signal during turnover of the enzyme by xanthine.[3d,5,6a] The very rapid signal has the most anisotropic $g$ matrix oserved for a XO signal, with $g_1$ greater than that of the free electron (Figure 12b, Table IV). $^1H$ coupling is absent, but strong, anisotropic coupling to $^{17}O$ ($\langle A \rangle$ = 1.37 mT) is observed. The data have been interpreted in terms

**Scheme III**

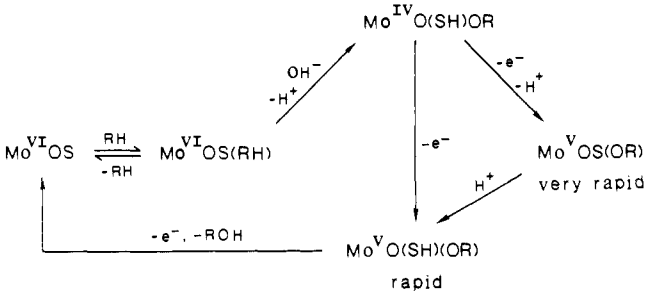


of a $Mo^{V}OS(OR)$ center[3d] (OR is the uric acid anion product obtained by oxidation of the C-8 position of xanthine).

While $\langle g \rangle$ for $[MoOSL]^-$ is lower than $\langle g \rangle$ for the very rapid XO signal (a result, primarily, of a low $g_3$) $g_1$ approaches that of $g_1$ for the enzyme and, importantly, exceeds $g$ of the free electron. These observations suggest $Mo^{V}OS$ as a reasonable candidate for the very rapid signal producing center.

$^{17}O$ coupling in $[Mo^{17}OSL]^-$ is small ($\langle A(^{17}O) \rangle = 0.43$ mT) but anisotropic (Table III) and can be compared to that in $[Mo^{17}O(SPh)_4]^-$, *cis*-$Mo^{17}O(SH)L$, and the smaller $^{17}O$ coupling in *cis*-$Mo^{17}O(^{17}OH)L$ (Table III, IV). The isotropic $^{17}O$ coupling of 1.37 mT observed for the very rapid signal is plausibly assigned to bound product ($^{17}OR$), as postulated by Bray and George[3d] in a $Mo^{V}(OS)(OR)$ center, rather than to the terminal oxo ligand. No evidence for a terminal oxo exists in the very rapid signal center; coupling to the latter may prove difficult to detect by EPR in the enzymes, however, where multiple signals and low Mo(V) and $^{17}O$ concentrations obtain.[3d]

The present work provides a basis for a minimum reaction scheme for the Mo site in XO. This scheme (Scheme III), a modification of the scheme of Bray and George,[3d] incorporates their earlier suggestion that the Michaelis complex involves binding of xanthine via its N-9 atom to the anion binding site of the enzyme.[3e] Nucleophilic attack by $OH^-$ induces electron and C-8 proton transfer to give $Mo^{IV}O(SH)OR$ with bound (OR) product. In this respect, the most recent EXAFS results for the fully substrate reduced species of XO,[3c] presumed to be the Mo(IV) form corresponding to the very rapid signal, detected a single oxo and no sulfide ligands, while previous EXAFS results[3a] for the fully dithionite reduced species gave the same result. Electron transfer to the one-electron acceptor $Fe_2S_2$ centers (more rapid than turnover[23]) produces the very rapid $Mo^{V}OS(OR)$[3d] and rapid $Mo^{V}O(SH)OR$ species in sequence or, as preferred in Scheme III, by parallel paths.[24] Further electron transfer induces product elimination and regeneration of the $Mo^{VI}OS$ site.

The $g$ values for sulfite oxidase and nitrate reductase are significantly higher than those for *cis*-MoO(OH)L, possibly reflecting the presence of additional thiolate or thioether ligands in the enzymes.[3,5,6,7,17] The EPR spectrum of SO (low pH form) features $^1H$ coupling of 0.98 mT and $^{17}O$ coupling of 0.6 mT, suggesting, as with the XO slow signal, the presence of an OH ligand. Similar considerations apply to the low-pH signal from NR (*E. coli* and *C. vulgaris*) and the "signal *A*" from spinach NR (Table IV), although $^{17}O$ data for these enzymes are lacking. These low-pH forms are in protic equilibrium with high-pH forms ($pK = 8.2$ for SO and 8.3 for *E. coli* NR), which exhibit no strongly coupled protons.[25] It has been suggested[3a,b] that the conjugate base forms may be $Mo^{V}O_2$ centers. While the high-pH forms do have significantly lower $\langle g \rangle$ values than the low-pH forms,[6] as is found for $[MoO_2L]^-$ vs. MoO(OH)L, their EPR spectra do not exhibit the exceptionally large anisotropy (extremely low $g_3$ value) observed with $[MoO_2L]^-$. This may be a result of a significantly different geometry at the enzyme Mo(V) centers, or it may be evidence in favor of a recent proposal[25] suggesting the high pH form of the Mo(V) centers of these enzymes may, in fact, have no oxo groups, with the exchangeable proton in the low-pH forms coordinated to another ligand atom, possibly N, of molybdenum.

It is also of interest to note $F^-$, $SH^-$, and $OH^-$, when apparently present in the trans position (MoOXL), exhibit no measurable EPR couplings to Mo(V). Coupling constants for $^{19}F$ of 0.77 mT have been reported for nitrate reductase from *E. coli*,[26] and 0.53 mT for sulfite oxidase[6b] while *cis*-MoOFL′ (L′$H_2$ = *N*,*N*′-dimethyl-*N*,*N*′-bis(2-hydroxybenzyl)ethylenediamine) shows $^{19}F$ coupling of 1.5 mT,[11] suggesting the $^{19}F$ coupling in the enzymes arises from a cis F ligand, possibly in a considerably distorted octahedral site.

## Experimental Section

**Materials.** Tetraethylammonium chloride, tetra-*n*-butylammonium perchlorate, tetra-*n*-butylammonium fluoride, and 2-benzothiazolol were obtained from Eastman; tetra-*n*-butylammonium tetrafluoroborate, tetra-*n*-butylammonium borohydride, sodium cyanoborohydride, glyoxal, benzylchloride, tetra-*n*-butylammonium hydroxide, $^2H_2O$ (100 atom % $^2H$), $CF_3COOH$ and $CF_3COO^2H$ (99 atom % $^2H$) from Aldrich; tetra-*n*-butylammonium hydrogen sulfide from Fluka; $Na_2MoO_4 \cdot 2H_2O$ from Fisher, and $H_2{}^{17}O$ (12.95 atom % $^{16}O$, 51.48 atom % $^{17}O$, 35.57 atom % $^{18}O$) from Mound Isotopes Laboratory. Reagent grade solvents, distilled and dried by standard methods, were used in all cases.

$[n\text{-}Bu_4N]_4Mo_8O_{26}$,[27] $(NH_4)_2MoOCl_5$,[28] $MoO_2(acac)_2$,[29] 2-methylbenzothiazolone,[30] and *N*-methyl-2-mercaptoaniline[31] were prepared by literature methods and characterized accordingly.

***N*,*N*′-Dimethyl-*N*,*N*′-bis(2-mercaptophenyl)ethylenediamine ($LH_2$).** *N*-Methyl-2-mercaptoaniline (13.9 g, 0.10 mol) in 125 mL of 2 N NaOH and 150 mL of EtOH was stirred with 13.9 g (0.11 mol) of benzyl chloride for 8 h at room temperature. EtOH was removed under vacuum, and the yellow liquid which separated from the solution was extracted with 3 × 50 mL portions of ethyl acetate. The extracts were combined and dried over anhydrous $MgSO_4$, the solvent removed with a rotary evaporator, and the oily liquid dried under vacuum at room temperature to give *N*-methyl-2-*S*-benzylthioaniline (I). Yield 98%.

*N*,*N*′-Dimethyl-*N*,*N*′-bis(2-*S*-benzylthiophenyl)ethylenediamine (II) was prepared from I and glyoxal following a sodium cyanoborohydride reductive amination procedure.[31] Glyoxal (5.20 g, 0.09 mol) was added to a solution of I (10.2 g, 0.045 mol) in 40 mL of MeOH. A solution of anhydrous $ZnCl_2$ (3.11 g, 0.025 mol) and $NaBH_3CN$ (2.78 g, 0.05 mol) in 75 mL of MeOH was added dropwise with stirring at room temperature. The mixture was stirred for 3 h (stirring time is most important: shorter times reduce the yield considerably while longer times give unknown side products). The off-white solid which precipitated was filtered, washed with 200 mL of MeOH, 1 L of hot (70 °C) $H_2O$, 200 mL of MeOH, and 200 mL of $Et_2O$ in turn and dried in vacuo at room temperature overnight. The product was dissolved in 80 mL of boiling *n*-butyl alcohol and 2.50 g (0.11 mol) of Na in small portions was added slowly. When the Na was completely dissolved, the solution was cooled and the pure white product filtered off, washed with 100 mL of MeOH, 500 mL of hot (70 °C) $H_2O$, and 100 mL MeOH in turn, and dried in vacuo at room temperature. Yield 28%; mp 178 °C.

$LH_2$ was obtained by addition of 4.84 g (0.01 mol) of II to 200 mL of *n*-butyl alcohol, to which freshly cut Na (4.60 g, 0.20 mol) was added in small portions and the suspension refluxed for 4 h. After being cooled, the solution was filtered and the filtrate extracted with 3 × 75 mL portions of $H_2O$. The solution was cooled to 0 °C and neutralized with 1:1 HCl. The white solid which separated was filtered, washed with 4 × 25 mL portions of $H_2O$, and dried in vacuo. Yield 65%; mp 92 °C. Anal. Calcd for $C_{16}H_{20}N_2S_2$: C, 63.12; H, 6.62; N, 9.22; S, 21.06. Found: C, 63.10; H, 6.59; N, 9.22; S, 21.15. IR: $\nu$(SH) 2540 $cm^{-1}$ (s). $^1H$ NMR ($CDCl_3$): 7.60–7.30 (m, Ph, 8 protons), 5.00 (s, SH, 2 protons), 3.10 (s, $-CH_2-CH_2-$, 4 protons), 2.68 ppm (s, $N-CH_3$, 6 protons).

(23) Olson, J. S.; Ballou, D. P.; Palmer, G.; Massey, V. *J. Biol. Chem.* **1974**, *249*, 4363.
(24) Tsopanakis, A. D.; Tanner, S. J.; Bray, R. C. *Biochem. J.* **1978**, *175*, 875. These results indicate the very rapid and rapid signals are not in protic equilibrium.
(25) Bray, R. C. *Polyhedron* **1986**, *5*, 591.
(26) George, G. N.; Bray, R. C.; Morpeth, F. F.; Boxer, D. H. *Biochem. J.* **1985**, *227*, 925.
(27) Fuchs, J.; Hartyl, H. *Angew. Chem., Int. Ed. Engl.* **1976**, *15*, 375. Shum, W. *J. Am. Chem. Soc.* **1976**, *98*, 8291.
(28) Palmer, W. G. *Experimental Inorganic Chemistry*; Cambridge University Press: Cambridge, U.K. **1934**; p 408.
(29) Chen, G. J.-J.; McDonald, J. W.; Newton, W. E. *Inorg. Chem.* **1976**, *15*, 2612.
(30) Hunter, R. F. *J. Chem. Soc.* **1930**, 125.
(31) Fujii, K. *J. Pharm. Soc. Jpn.* **1957**, *77*, 3.
(32) Kim, S.; Ho Oh, C.; Sukko, J.; Ahn, K. H.; Kim, Y. J. *J. Org. Chem.* **1985**, *50*, 1927.

**Table V.** Summary of Crystal and Refinement Data for $MoN_2O_2S_2C_{16}H_{18}$

| | |
|---|---|
| space group | $P2_1/n$ |
| $a$, Å | 10.049 (2) |
| $b$, Å | 14.538 (2) |
| $c$, Å | 12.143 (1) |
| $\beta$, deg | 103.73 (1) |
| $V$, Å$^3$ | 1723.3 |
| $Z$ | 4 |
| fw, daltons | 430.40 |
| $D_{calcd}$, g cm$^{-3}$ | 1.66 |
| radiation, Å | Mo K$\alpha$ ($\lambda$ = 0.71073) |
| temp, °C | 23 ± 1 |
| $\mu$, cm$^{-1}$ | 9.8 |
| scan type | $\theta/2\theta$ |
| scan speed, deg min$^{-1}$ | 2.0–8.0 |
| scan width, deg | (2$\theta$K$\alpha_1$ − 0.9) to (2$\theta$K$\alpha_2$ + 1.5) |
| max 2$\theta$, deg | 60.0 |
| unique reflections | 5046 |
| unique data used | 3902 with $F_o^2 > 3.0\sigma(F_o^2)$ |
| $R$ | 0.031 |
| $R_w$ | 0.041 |
| GOF[a] | 1.39 |

[a] GOF = $[\sum w(|F_o| - |F_c|)^2/(NO - NV)]^{1/2}$; $R = \sum(|F_o| - |F_c|)/\sum|F_o|$; $R_w = [\sum w(|F_o| - |F_c|)^2/\sum wF_o^2]^{1/2}$. NO = number of observations; NV = number of variables.

**$MoO_2L$. Method 1.** [$n$-Bu$_4$N]$_4$Mo$_8$O$_{26}$ (1.00 g, 0.46 mmol) was dissolved in 25 mL of hot MeOH. The solution was cooled to 0 °C and 1.06 g (3.48 mmol) of $LH_2$ in 5 mL of $CH_2Cl_2$ was added dropwise with stirring. The solution was stirred for 4 h, after which the red-brown solid which formed was collected by filtration, washed with 5 × 20 mL portions of MeOH, and dried in vacuo. Yield 82%. The compound was recrystallized from $CHCl_3/Et_2O$ (1:2) at room temperature and dried in air to give red crystals. Anal. Calcd for $MoC_{16}H_{18}N_2O_2S_2$: C, 44.65; H, 4.22; N, 6.51; S, 14.90. Found: C, 44.54; H, 4.29; N, 6.62; S, 14.71. $\nu$(Mo=O) 912 and 880 cm$^{-1}$.

**Method 2.** $LH_2$ (0.046 g, 0.15 mmol) dissolved in 0.5 mL of deaerated $CH_2Cl_2$ was added to a solution of 0.05 g (0.15 mmol) of $MoO_2(acac)_2$ in 5 mL of MeOH and the solution stirred under $N_2$ for 1 h. The red-brown precipitate was filtered, washed with 5 mL of MeOH and 20 mL of $Et_2O$, and dried under vacuum at room temperature. Yield 80%.

**$Mo^{17}O_2L$ and $^{98}Mo^{17}O_2L$.** Complexes enriched to 50 atom % in $^{17}O$ were prepared according to method 2 from $Mo^{17}O_2(acac)_2$ (50 atom % $^{17}O$). The $^{17}O$-substituted $MoO_2(acac)_2$ was prepared as follows: $Na_2MoO_4{\cdot}2H_2O$ (0.132 g, 0.55 mmol) was incubated anaerobically with 1.2 mL of $H_2O$ ($^{16}O$:$^{17}O$:$^{18}O$ = 12.95:51.48:35.57 atom %) overnight. Freshly distilled acetylacetone (0.20 mL) was added, followed by HCl (0.16 mL, 6.2 M, same isotope concentration of $H_2O$ as above) slowly and dropwise until precipitation of the product commenced at pH 2.0. The mixture was stirred for 24 h with periodic checking of the pH. The product was filtered, washed with $H_2O$, $n$-BuOH, and cold $Et_2O$, and dried under vacuum. Yield 0.18 g (75%). $\nu$(Mo=O): 924, 909, 903, 886, 870 cm$^{-1}$; 935, 906 cm$^{-1}$ for $Mo^{16}O_2(acac)_2$. Complexes enriched to 96 atom % in $^{98}$Mo employed $Na_2{}^{98}MoO_4{\cdot}2H_2O$ prepared by the method of ref 21.

**MoOClL.** All operations were carried out under an atmosphere of dry prepurified $N_2$ with deaerated solvents in Schlenk apparatus. A solution of $LH_2$ (0.35 g, 1.10 mmol) in 10 mL of $CH_2Cl_2$ was added dropwise with stirring to 0.33 g (1.0 mmol) of $(NH_4)_2MoOCl_5$ in dry MeOH. The deep blue-green solution was stirred for 12 h and the solvent removed under vacuum. The solid was dissolved in 25 mL of $CH_2Cl_2$ and the $NH_4Cl$ filtered off. The filtrate was concentrated to 10 mL and stirred at −20 °C overnight. Dark blue-green microcrystals separated and were collected by filtration and dried under vacuum. Yield 80%. The product was recrystallized from $CH_2Cl_2$/MeOH at −20 °C, giving shining dark blue-green microcrystals. Anal. Calcd for Mo $C_{16}H_{18}N_2ClOS_2$: C, 42.72; H, 4.00; N, 6.23; Cl 7.88; S, 14.25. Found: C, 42.82; H, 4.13; N, 6.23; Cl, 7.74; S, 14.46. $\nu$(Mo=O) 948 cm$^{-1}$.

**Collection and Processing of Crystallographic Data.** Suitable crystals of $MoO_2L$ were grown from 1:2 $CHCl_3/Et_2O$ at room temperature. A crystal of dimensions 0.54 × 0.13 × 0.33 mm was examined with a Nicolet Syntex $P2_1$ X-ray diffractometer equipped with a graphite crystal incident beam monochromator. The mosaicity was satisfactory (0.29°); other crystallographic data are summarized in Table V. Three representative reflections were measured every 46 reflections. The intensities of these standard reflections remained constant within experimental error, and no decay correction was required. Lorentz and polarization corrections were applied to the data. No absorption correction was applied because the linear absorption coefficient is only 9.8 cm$^{-1}$, and several $\psi$-scans indicated that the relative absorption correction varied less than 5%.

**Table VI.** Electronic Spectroscopic Data[a]

| complex | max, nm | log $\epsilon$ |
|---|---|---|
| $MO_2L$ | 412 | 3.70 |
| *trans*-MoOClL[b] | 680 sh | |
| | 575 | 3.39 |
| | 430 sh | |
| | 375 | 3.42 |
| $[MoO_2L]^-$[b] | 460 | 2.29 |
| | 380 | 3.29 |
| $[MoO(S)L]^-$[b,c] | 461 | 3.78 |
| *trans*-MoO(OH)L[d] | 510 | 3.28 |
| | 410 | 3.36 |
| *trans*-MoOFL[d] | 550 | 3.30 |
| | 390 | 3.38 |

[a] MeCN. [b] 0.10 M [$n$-Bu$_4$N][BF$_4$]. [c] Excess [$n$-Bu$_4$N]SH present. [d] Excess anion present.

**Table VIIa.** Positional Parameters for $MoO_2L$[a]

| atom | $x$ | $y$ | $z$ | $B_{eq}$, Å$^2$ |
|---|---|---|---|---|
| Mo | 0.02152 (2) | −0.17943 (1) | 0.24985 (2) | 2.864 (4) |
| S1 | −0.09349 (7) | −0.32487 (5) | 0.20267 (5) | 3.62 (1) |
| S2 | 0.19263 (7) | −0.06913 (4) | 0.33969 (7) | 3.60 (1) |
| O1 | 0.0147 (2) | −0.1632 (2) | 0.1103 (2) | 4.64 (5) |
| O2 | −0.1015 (2) | −0.1123 (2) | 0.2832 (2) | 4.68 (5) |
| N2 | 0.2333 (2) | −0.2680 (1) | 0.2785 (2) | 2.41 (3) |
| N1 | 0.0490 (2) | −0.2538 (1) | 0.4359 (2) | 2.40 (3) |
| C1 | −0.1223 (2) | −0.3639 (2) | 0.3316 (2) | 2.78 (4) |
| C2 | −0.2209 (3) | −0.4320 (2) | 0.3298 (2) | 3.58 (5) |
| C3 | −0.2476 (3) | −0.4633 (2) | 0.4297 (3) | 4.07 (6) |
| C4 | −0.1746 (3) | −0.4298 (2) | 0.5320 (3) | 4.13 (6) |
| C5 | −0.0738 (3) | −0.3639 (2) | 0.5355 (2) | 3.37 (5) |
| C6 | −0.0504 (2) | −0.3285 (2) | 0.4348 (2) | 2.52 (4) |
| C7 | 0.0351 (3) | −0.1830 (2) | 0.5215 (2) | 3.53 (5) |
| C8 | 0.1918 (2) | −0.2917 (2) | 0.4676 (2) | 2.71 (4) |
| C9 | 0.2275 (2) | −0.3382 (2) | 0.3675 (2) | 2.64 (4) |
| C10 | 0.2348 (3) | −0.3152 (2) | 0.1690 (2) | 3.63 (5) |
| C11 | 0.3591 (2) | −0.2135 (2) | 0.3137 (2) | 2.57 (4) |
| C12 | 0.4867 (2) | −0.2531 (2) | 0.3230 (2) | 3.45 (5) |
| C13 | 0.6048 (3) | 0.2002 (2) | 0.3518 (3) | 4.25 (6) |
| C14 | 0.5956 (3) | −0.1076 (2) | 0.3728 (3) | 4.28 (6) |
| C15 | 0.4700 (3) | −0.0682 (2) | 0.3680 (2) | 3.78 (5) |
| C16 | 0.3506 (2) | −0.1209 (2) | 0.3388 (2) | 2.82 (4) |

The structure was solved by the heavy atom Patterson method which revealed the position of the Mo atom. The remaining atoms were located in succeeding difference electron density maps. Hydrogen atoms were included in the final refinement but restrained to ride on the atom to which they are bonded. The C–H bond lengths were fixed at 0.95 Å. The function minimized was $\sum w(|F_o - F_c|)^2$, with $w = 4F_o^2/[\sigma^2(F_o^2) + (pF_o^2)^2]$ and $p = 0.04$. Scattering factors were from Cromer and Waber.[33] The effects of anomalous dispersion were included in $F_c$.[34,35] All calculations were performed on a PDP-11/34a computer with use of SDP-PLUS.[36] Fractional coordinates appear in Table VII.

**Electrochemistry.** Cyclic voltammetry and coulometry were performed in MeCN, DMF (Burdick and Jackson, dried over molecular sieves), or THF (distilled) with [$n$-Bu$_4$N][BF$_4$], [$n$-Bu$_4$N]ClO$_4$, or [Et$_4$N]Cl (recrystallized 3 times) as electrolyte. Data were obtained at room temperature with use of a three-electrode cell described previously[37] and a PAR Model 173 potentiostat, equipped with a digital coulometer, 174 polarographic analyzer, and 175 signal generator. Potential measurements were made with the SCE as reference and have a precision of ±0.005 V; coulometric measurements were made at a potential 0.10 V

(33) Cromer, D. T.; Waber, J. T. *International Tables for X-Ray Crystallography*; The Kynoch Press: Birmingham, England, 1974; Vol. IV, Table 2.2B.
(34) Ibers, J. A.; Hamilton, W. C. *Acta Crystallogr.* **1964**, *17*, 871.
(35) Cromer, D. T. *International Tables for X-Ray Crystallography*; The Kynoch Press: Birmingham, England, 1974; Vol. IV, Table 2.3.1.
(36) Frenz, B. A. In *Computing in Crystallography*; Schenk, H., Olthof-Hazelkamp, B., von Konigsveld, H., Bassi, G. C., Eds.; Delft University Press: Delft, Holland, 1978; pp 64.71.
(37) Taylor, R. D.; Street, J. P.; Minelli, M.; Spence, J. T. *Inorg. Chem.* **1978**, *17*, 3207.

more negative than the CV reduction peak with a precision for $n$ of ±10%.

Reductions at −42 °C in THF were performed in a specially designed cell directly in the EPR cavity,[38] using a BAS SP-2 Potentiostat and a BAS CV-27 voltammograph. Temperature was maintained by flow of $N_2$ cooled by liquid $N_2$ through a Varian temperature dewar insert and controlled by a Delton TM-20 temperature controller. Temperature was monitored with a calibrated digital thermocouple in the electrochemical cell.

**EPR.** EPR spectra were obtained with a Varian E-109 X-band spectrometer, equipped with a variable-temperature dewar insert and temperature controller. Samples from room temperature reductions were transferred with a gas tight syringe under Ar or $N_2$ from the coulometer cell to a flat cell for room temperature spectra or to an EPR tube and frozen immediately in liquid $N_2$ for frozen spectra. For EPR measurements at −78 °C in THF, samples were transferred with a gas tight syringe from the reaction flask immersed in dry ice–acetone to an EPR tube, frozen immediately in liquid $N_2$ and sealed under vacuum. They were allowed to warm to −78 °C in the variable-temperature dewar in the EPR cavity and the spectra recorded.

EPR spectra at −42 °C in THF were obtained by electrochemical reduction of $1.00 \times 10^{-2}$ M solutions of $MoO_2L$ directly in the EPR cavity (vide supra). Reduction was continued until the spectra ceased growing. Frozen spectra (−135 °C) were obtained by lowering the temperature of the cell after reduction at −42 °C.

$[MoOL]^+$ (deep violet) was obtained by addition of 2 equivs of $CF_3COOH$ to a solution of $[MoO_2L]^-$. $[MoO(S)L]^-$ (orange brown) was obtained by addition of 10-fold excess of $[n\text{-}Bu_4N]SH$ to a solution of MoOClL in THF. *cis*-MoO(SH)L (light blue) was obtained by cooling the solution of $[MoO(S)L]^-$ to −78 °C in a dry ice/acetone bath followed by addition of a 5–10-fold excess of $CF_3COOH$ at −78 °C (color change from orange brown to blue). *cis*-$MoO(S^2H)L$ was prepared in the same way with $CF_3COO^2H$ in $^2H_2O$ (1.5 M). *trans*-MoO(SH)L (grey brown) was obtained by the warming of the *cis*-MoO(SH)L solution to room temperature, by addition of excess $CF_3COOH$ to $[MoO(S)L]^-$ at room temperature, or by addition of 1.5 equiv of $[n\text{-}Bu_4N]SH$ to MoOClL at room temperature. *trans*-MoO(OH)L (rose) was prepared by addition of 2.5 equiv of $[n\text{-}Bu_4N]OH$ to a solution of MoOClL. *trans*-MoOFL (deep blue) was obtained by preparation of a solution of MoOClL in 0.10 M $[n\text{-}Bu_4N]F$.

EPR ($g$), $^{95,97}Mo$ ($A$), and $^1H$ ($A$) values (Table III) were obtained from the solution spectra, using DPPH as standard. Anisotropic $g$ and $A$ values and $^{17}O$ ($A$) values (Table III) were determined by computer simulation, using a program developed by White and Belford[39] and modified by White et al.[40] The program was obtained from N. D. Chasteen, Department of Chemistry, University of New Hampshire. The program has provision for one angle of noncoincidence between $g$ and $A$ tensors. The program was run on an IBM PC computer equipped with a 8087 math processor. Spin concentrations were estimated with *cis*-$MoOCl(tox)_2$ as standard, with a precision of ±15%.

While the geometry of the Mo(V) complexes has not been determined, it is unlikely their symmetry is higher than $C_2$ ($[MoO_2L]^-$, $[MoOL]^+$), $C_s$ (*trans*-MoOXL: X = Cl, F, SH, OH)) or $C_1$ (*cis*-MoO(OH)L, *cis*-MoO(SH)L, $[MoOSL]^-$). For $C_2$ and $C_s$ one coincidence of the $g$ and $A$ ($^{95,97}Mo$) tensors is required; in $C_1$ none need be coincident. Because of the complicated relationships between $g$ and $A$ ($^{95,97}Mo$) tensors for complexes apparently having more than one noncoincidence, it is not possible to obtain anisotropic $A$ values from the data. This requires multifrequency measurements and a simulation program providing for three noncoincident angles.

Satisfactory simulations of the $I = 0$ and $^5/_2$ features of the EPR spectra for $[MoO_2L]^-$, $[MoO(S)L]^-$, *trans*-MoOClL, *trans*-MoOFL, and *trans*-MoO(OH)L were obtained with the parameters in Table III. Satisfactory simulations for the $I = {}^5/_2$ features of *cis*-MoO(OH)L, $[MoOL]^+$, *cis*-MoO(SH)L, and *trans*-MoO(SH)L could not be obtained; only ($A(^{95,97}Mo)$) values appear in Table III for these complexes.

**Acknowledgment.** Financial support for this work by National Science Foundation Grant CHE-8402136 and National Institute of Health Grant GM 08347 (J.T.S.), the Australian Research Grants Scheme (A.G.W.), and National Institutes of Health Grant GM 37773 (J.H.E.) is gratefully acknowledged. The Ministry of Education and Culture and R.R.L. Jorhat, Assam, India, are thanked for granting leave to D.D.

**Registry No.** I, 109334-46-5; II, 109334-47-6; $LH_2$, 109334-45-4; XO, 9002-17-9; SO, 62079-39-4; NR, 9013-03-0; $MoO_2L$, 109309-12-8; $MoO_2(acac)_2$, 17524-05-9; *trans*-MoOClL, 109309-13-9; $[MoO_2L]^-$, 109309-14-0; $[MoOL]^+$, 109309-15-1; *cis*-MoO(OH)L, 109309-16-2; $[MoOSL]^-$, 109309-17-3; *cis*-MoO(SH)L, 109309-18-4; *trans*-MoO(OH)L, 109428-93-5; *trans*-MoOFL, 109309-19-5; *trans*-MoO(SH)L, 109428-94-6; $Mo^{17}O_2L$, 109309-20-8; $^{98}Mo^{17}O_2L$, 109309-21-9; $Mo^{17}O_2(acac)_2$, 109309-22-0; $NaBH_3CN$, 25895-60-7; $[(n\text{-}Bu_4)N]_4Mo_8O_{26}$, 61245-60-1; $(NH_4)_2MoOCl_5$, 17927-44-5; $Na_2{}^{98}MoO_4$, 109309-23-1; *N*-methyl-2-mercaptoaniline, 21749-63-3; benzyl chloride, 100-44-7; glyoxal, 107-22-2.

**Supplementary Material Available:** Listings of idealized hydrogen atom positions (Table VIIb), additional bond distances and angles (Table VIII), and thermal parameters for $MoO_2L$ (Table IX) (4 pages); listings of structure factors for $MoO_2L$ (9 pages). Ordering information is given on any current masthead page.

(38) Bagchi, R. N.; Bond, A. M.; Colton, R. *J. Electroanal. Chem.*, in press.
(39) White, L. K.; Belford, R. L. *J. Am. Chem. Soc.* **1976**, *98*, 4428.
(40) White, L. K.; Albanese, N.; Chasteen, N. D., unpublished work.
(41) Gutteridge, S.; Bray, R. C. *Biochem. J.* **1980**, *189*, 615.
(42) Malthouse, J. P. G.; Williams, J. W.; Bray, R. C. *Biochem. J.* **1981**, *197*, 421.
(43) Hawkes, T. R.; George, G. N.; Bray, R. C. *Biochem. J.* **1984**, *218*, 961.